

*Rapid Commun. Mass Spectrom.* 2016, 30, 379–385  
(wileyonlinelibrary.com) DOI: 10.1002/rcm.7447

# Cluster secondary ion mass spectrometry imaging of interfacial reactions of TiO<sub>2</sub> microspheres embedded in ionic liquids

Kan Shen\*, Jay G. Tarolli and Nicholas Winograd

Department of Chemistry, The Pennsylvania State University, University Park, Pennsylvania 16802, USA

**RATIONALE:** Our goal is to develop protocols for the elucidation of the identity and structure of reaction products embedded in a reaction medium. Results should find significance in a variety of disciplines ranging from the study of biological cells and tissues, to the steps associated with the functionalization of nanoparticles.

**METHODS:** We utilize cluster secondary ion mass spectrometry (cluster-SIMS) to acquire three-dimensional (3D) information about 5–30 μm TiO<sub>2</sub> microspheres imbedded into an ionic liquid. The method allows molecular depth profiling with submicron spatial resolution and depth profiling with a resolution of several tens of nanometers. The ionic liquid matrix enshrouds the spheres, allowing them to be introduced into the vacuum environment of the mass spectrometer.

**RESULTS:** The results provide 3D chemical information about these microspheres as they are synthesized by interfacial sol-gel reactions. We show that with 40 keV C<sub>60</sub><sup>+</sup>, it is possible to erode through the reaction medium and map the distribution of those embedded TiO<sub>2</sub> microspheres. Moreover, we demonstrate that it is possible to monitor surface modification of the particles and, via ion beam drilling, elucidate their internal structure.

**CONCLUSIONS:** Using cluster-SIMS imaging, we are able to elucidate the identity and structure of reaction products embedded in a reaction medium, a problem of long-standing interest for materials characterization. With this strategy, we have provided a new approach that may be especially useful for the characterization of biological tissue and cells within the vacuum confines of the mass spectrometer. Copyright © 2015 John Wiley & Sons, Ltd.

Elucidation of the identity and structure of reaction products embedded in a reaction medium has long proven to be a difficult challenge for materials characterization. The challenge is found in a variety of disciplines ranging from the study of reactions in biological cells and tissue,<sup>[1,2]</sup> to the steps associated with the functionalization of nanoparticles.<sup>[3,4]</sup> Cluster secondary ion mass spectrometry (cluster-SIMS) is an emerging methodology that provides chemical imaging information with sub-micron resolution and depth resolution of several tens of nanometers.<sup>[5–7]</sup> This level of highly specific three-dimensional (3D) chemical information is a unique capability. A major complicating factor in the widespread application of this technique is, with a notable exception,<sup>[8]</sup> that experiments must be carried out in a high vacuum environment. For the characterization of single cells, for example, the samples need to be chemically fixed,<sup>[9,10]</sup> or frozen<sup>[11–14]</sup> to reduce vapor pressure and vacuum-induced chemical and structural changes.

Because of sample preparation issues, especially for biomaterials, ambient pressure mass spectrometer methods have become popular. One approach, desorption electrospray ionization (DESI),<sup>[15]</sup> has been successfully applied in the imaging modality to a wide range of biological tissues.<sup>[16,17]</sup>

There are limits to the spatial resolution to ~20 μm, however, that still restrict the range of applications. With SIMS, it has been possible to examine samples in liquid solution by the creation of a micron-size hole through which the beam is directed, but imaging quality is also more difficult.<sup>[8]</sup> Another option is to employ ionic liquids,<sup>[18–20]</sup> salts in which the ions are weakly coordinated with each other. Two unique features of these liquids are that their properties can be tuned by proper selection of the component ions and that they have negligible vapor pressure. The combination of SIMS and ionic liquids can be mutually beneficial. For example, ionic liquids could be used as a reaction medium and/or matrix to preserve analytes of interest in vacuum condition for SIMS analysis, greatly extending the scope of SIMS applications. Until now, however, the major application of ionic liquids for SIMS has been as matrices to enhance ionization.<sup>[21–23]</sup>

In this study, we performed depth profiling and chemical imaging with SIMS to detect reactions which occur in ionic liquids. The model system is comprised of TiO<sub>2</sub> microspheres with diameters of 5–30 μm formed by interfacial sol-gel reactions in an ionic liquid. The results show that 40 keV C<sub>60</sub><sup>+</sup> ions are able to erode through the reaction medium and map the distribution of those embedded TiO<sub>2</sub> microspheres. The results also show that SIMS is capable of detecting surface modification of these microspheres as well as probing into the interior of the spheres. In general, we have developed a SIMS protocol for the direct analysis of reactions that use ionic liquids as an embedding medium.

\* Correspondence to: K. Shen, Department of Chemistry, The Pennsylvania State University, University Park, Pennsylvania 16802, USA.  
E-mail: kan.shen1985@gmail.com

## EXPERIMENTAL

### Preparation of hollow TiO<sub>2</sub> microspheres

A slightly modified version of the hollow metal oxide microspheres synthesis method described by Nakashima *et al.*<sup>[24]</sup> was employed in the preparation of hollow TiO<sub>2</sub> microspheres. A schematic illustration of the formation process is shown in Fig. 1. In brief, 1 mL of 1-butyl-3-methylimidazolium hexafluorophosphate (BMIM-PF<sub>6</sub>) (Matrix Scientific, Columbia, SC, USA) was added into a 20-mL glass scintillation vial, dried in an oven at 120 °C for 2 h, and then allowed to cool to room temperature in a desiccator prior to use. Next, 0.2 mL anhydrous toluene solution containing 0.3 M titanium tetra-*n*-butoxide (Ti(OBu)<sub>4</sub>) (Acros Organics, Fair Lawn, NJ, USA) was added dropwise into the ionic liquid, and the mixture was then stirred at 800 rpm for 5 min at room temperature. Hollow TiO<sub>2</sub> microspheres with a diameter of 5–30 μm were formed via interfacial hydrolysis and condensation reactions between Ti(OBu)<sub>4</sub> dissolved in toluene droplets and trace water adsorbed in BMIM-PF<sub>6</sub>.<sup>[24]</sup>

### Preparation of fluorescent-labeled hollow TiO<sub>2</sub> microspheres

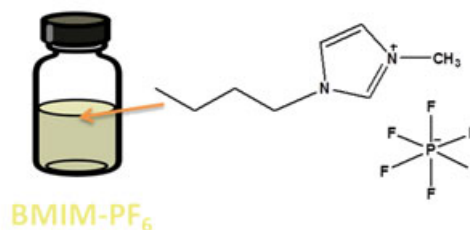
For synthesis of fluorescent-labeled hollow TiO<sub>2</sub> microspheres,<sup>[24]</sup> 1 mL of BMIM-PF<sub>6</sub> was treated following the recipe described above. The glass vial containing the ionic liquid was then wrapped in foil and kept in darkness. Next, 0.1 mg fluorescein isothiocyanate (FITC) (Fisher Scientific, Pittsburgh, PA, USA) and 0.2 mL anhydrous toluene solution containing 0.3 M Ti(OBu)<sub>4</sub> were added sequentially into the ionic liquid and the resulting mixture was stirred at 800 rpm for 5 min at room temperature. Hollow TiO<sub>2</sub> microspheres coated with fluorescent dyes were formed, as shown in Fig. 2(a). A possible binding mechanism, as depicted in Fig. 2(b), is that the carboxyl group of FITC dyes can simultaneously interact with the surface of TiO<sub>2</sub> microspheres by bidentate chelation or the formation of a bidentate bridge as the hollow TiO<sub>2</sub> microspheres form.<sup>[25,26]</sup>

### SIMS and SEM analyses

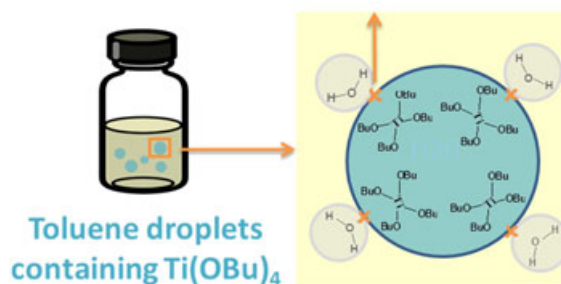
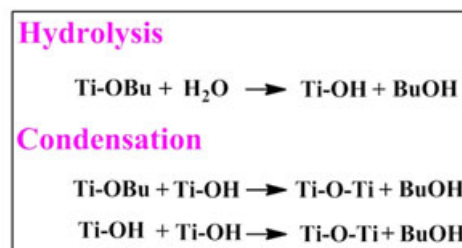
Sample analysis was performed using a J105 3D Chemical Imager (Ionoptika Ltd, Southampton, UK), the design of which has been described in detail elsewhere.<sup>[27]</sup> The instrument is equipped with a 40 kV C<sub>60</sub> primary ion beam. Singly charged C<sub>60</sub><sup>+</sup> primary ions were selected by a Wien filter and were focused to provide approximately 1 pA beam current with a 1 μm beam diameter. The beam was directed toward the sample surface at an angle of 40° relative to the surface normal in continuous current mode, generating a continuous stream of secondary ions. The secondary ions were collected in a buncher and then accelerated into a time-of-flight (TOF) mass analyzer. All the experiments were performed at room temperature (RT) in the positive ion mode and the pressure of the analysis chamber was maintained at ~10<sup>-9</sup> Torr.

To characterize synthesized microspheres, 10 μL of the reaction solution was spread onto a 5 mm × 5 mm Si wafer by spin coating. The C<sub>60</sub><sup>+</sup> ion beam was used to depth profile through a small region of the sample and SIMS images of 256 × 256 pixels and corresponding mass spectra were

## (a) Reaction Medium



## (b) Interfacial Sol-Gel Reaction



## (c) Reaction Products

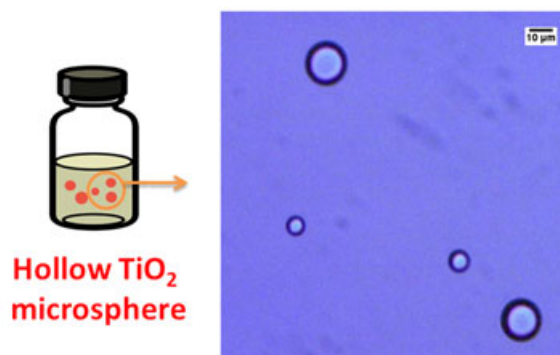


**Figure 1.** Schematic of the hollow TiO<sub>2</sub> microspheres formation process. (a) Structure of 1-butyl-3-methylimidazolium hexafluorophosphate (BMIM-PF<sub>6</sub>) ionic liquid. BMIM-PF<sub>6</sub> served as the reaction medium in this study. (b) Ti(OBu)<sub>4</sub> dissolved in toluene droplets reacted with trace water adsorbed in BMIM-PF<sub>6</sub> at the interface. Hollow TiO<sub>2</sub> microspheres were obtained via the interfacial sol-gel reaction. (c) Optical micrograph of the synthesized TiO<sub>2</sub> microspheres.

recorded for each layer. No sample charging was noticed in the positive SIMS mode and the acquired mass spectra have a mass resolution of 5000 (m/Δm).

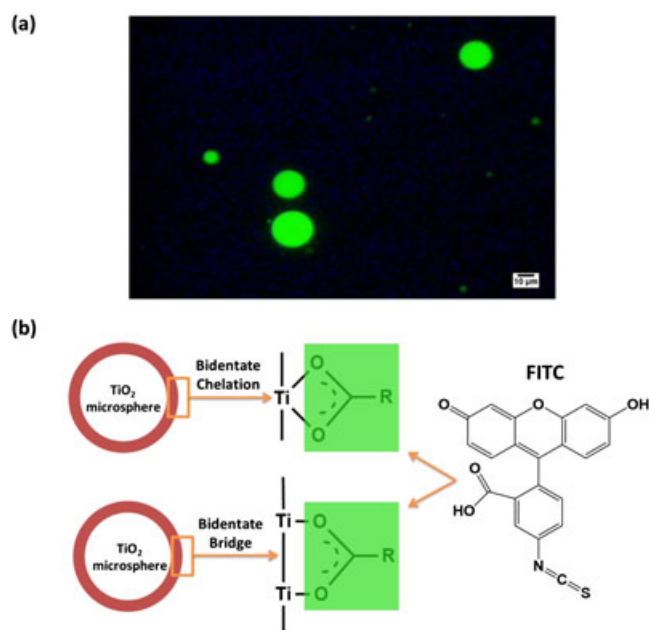


**Figure 2.** Surface modification of hollow TiO<sub>2</sub> microspheres by fluorescent dye FITC: (a) fluorescent micrograph of the FITC dyed hollow TiO<sub>2</sub> microspheres and (b) schematic of the binding of FITC dye with the surface of hollow TiO<sub>2</sub> microspheres.

In addition, the instrument is equipped with an electron detector, allowing the acquisition of scanning electron microscopy (SEM) images of 512 × 512 pixels. For the SEM measurement, 10 μL of reaction solution was first diluted 100-fold with methanol and then centrifuged at 2000 rpm for 5 min. The resulting pellet was resuspended in 100 μL methanol and then spin cast onto a 5 mm × 5 mm Si wafer. This sample preparation procedure removes most of the ionic liquid and helps identify the locations of the microspheres.

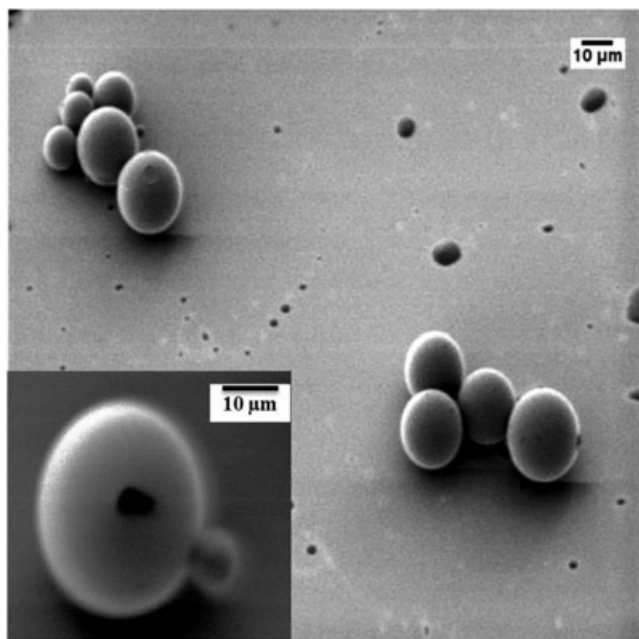


**Figure 3.** SEM image (512 × 512 pixels) of the synthesized hollow TiO<sub>2</sub> microspheres taken using a 40 keV C<sub>60</sub><sup>+</sup> primary ion source. The field of view for the image is 300 μm × 300 μm.

## RESULTS AND DISCUSSION

### SEM image of TiO<sub>2</sub> microspheres

A representative SEM image of the TiO<sub>2</sub> microspheres synthesized in the ionic liquid is shown in Fig. 3. It is clear that spheres which range in size from 5 μm to 30 μm could be detected with the C<sub>60</sub><sup>+</sup> primary ion beam. Note that the edges of the spheres appear brighter than the central part of the image. The effect arises since more secondary electrons escape from the edges of a sample than from flat areas.<sup>[28]</sup> The inset SEM image shows a sphere with a hole in it. Note that there are no secondary electrons coming out of the hole. This observation suggests that the microsphere has a hollow core.<sup>[24]</sup>

### Visualization of TiO<sub>2</sub> microspheres embedded in BMIM-PF<sub>6</sub> with image depth profiling by TOF-SIMS

With the 40 keV C<sub>60</sub><sup>+</sup> primary ion beam, a total ion fluence of 1.0 × 10<sup>15</sup> ions/cm<sup>2</sup> was applied to depth profile through an area of 70 μm × 70 μm. The dataset contains 20 images in total and all the images were taken at 256 × 256 pixels. The mass spectra corresponding to the first and the last image are shown in Fig. 4 and they look distinctly different. At the

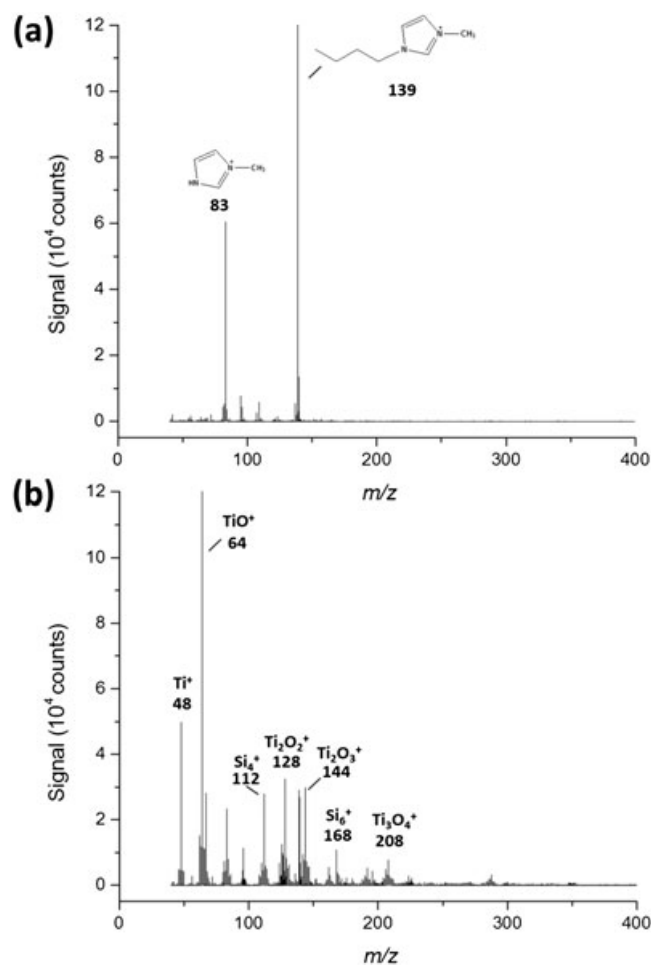


**Figure 4.** Image depth profiling through a region of interest with a total ion fluence of 1.0 × 10<sup>15</sup> ions/cm<sup>2</sup> C<sub>60</sub><sup>+</sup> bombardment: (a) and (b) are the mass spectra corresponding to the first and the last image, respectively.

beginning, the mass spectrum is dominated by peaks at  $m/z$  83 and 139 (Fig. 4(a)), which are the characteristic ions of BMIM-PF<sub>6</sub>. There is no indication for the existence of TiO<sub>2</sub> microspheres. However, after etching 20 layers, the signal of the ionic liquid largely disappeared, and peaks at  $m/z$  48, 64, 128, 144, and 208 for TiO<sub>2</sub> and at  $m/z$  112 and 168 for the Si substrate (Fig. 4(b)) became the main ions in the mass spectrum.

A chemical image for BMIM<sup>+</sup>, Ti<sub>2</sub>O<sub>3</sub><sup>+</sup> and Si<sub>6</sub><sup>+</sup> was then constructed for each layer to help visualize the change in the distributions as a function of C<sub>60</sub><sup>+</sup> ion fluence, as shown

in Fig. 5. The results show that at the beginning, the reaction solution was spread over the substrate, and the majority of the Si substrate was covered by ionic liquid. Through erosion, BMIM-PF<sub>6</sub> was gradually removed while the Ti<sub>2</sub>O<sub>3</sub><sup>+</sup> signal appears from the reaction medium. At the end of the depth profile, the Ti<sub>2</sub>O<sub>3</sub><sup>+</sup> signal is only distributed in four spherical-shaped areas with the remainder of the image area showing as Si. In addition, as seen in Fig. 6, the distributions of  $m/z$  48 for Ti<sup>+</sup>,  $m/z$  64 for TiO<sup>+</sup>,  $m/z$  128 for Ti<sub>2</sub>O<sub>2</sub><sup>+</sup>, and  $m/z$  208 for Ti<sub>3</sub>O<sub>4</sub><sup>+</sup> were colocalized with that of  $m/z$  144 for Ti<sub>2</sub>O<sub>3</sub><sup>+</sup>, which confirms that the microspheres are made of TiO<sub>2</sub>.

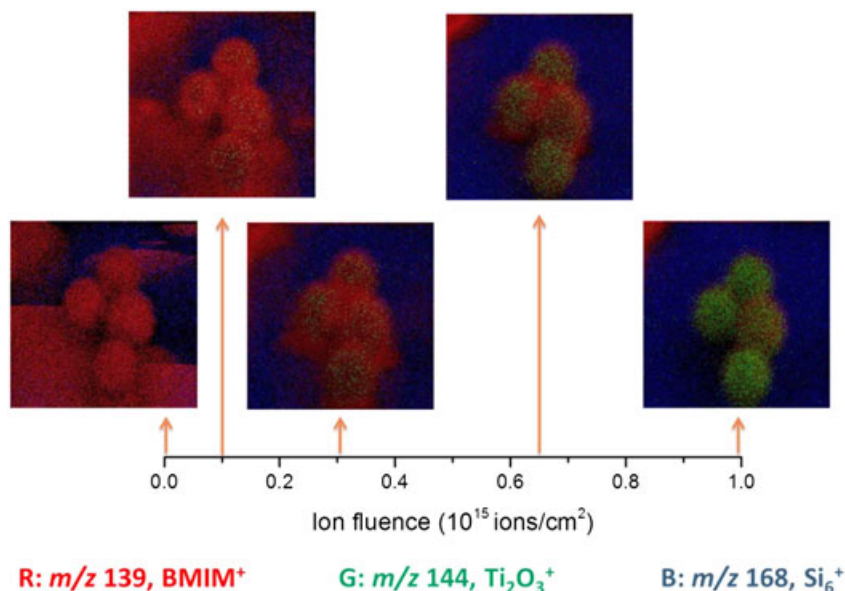


**Figure 5.** RGB overlay of BMIM<sup>+</sup> ( $m/z$  139, red), Ti<sub>2</sub>O<sub>3</sub><sup>+</sup> ( $m/z$  144, green) and Si<sub>6</sub><sup>+</sup> ( $m/z$  168, blue) to show the change in their distributions during the depth profiling process. All images are taken from a 70  $\mu\text{m} \times 70 \mu\text{m}$  area.

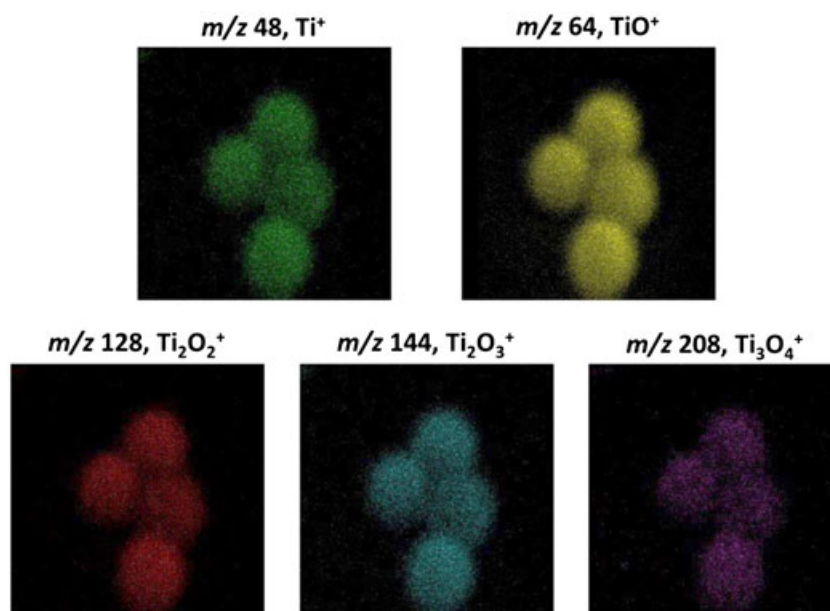


**Figure 6.** All TiO<sub>2</sub>-related peaks were colocalized.

### Hollow core of the TiO<sub>2</sub> microsphere

The next step was to investigate the internal structure of the TiO<sub>2</sub> microsphere. The bottom sphere of the four available ones, as shown above, was chosen to be the target of the analysis. Since it is known that the sputtering rate of inorganic materials is much slower than that of organic materials,<sup>[29]</sup> the 40 keV C<sub>60</sub><sup>+</sup> ion beam was chosen to etch through a small part (5 μm × 5 μm) of the sphere in DC mode and the etching process was stopped immediately after the disappearance of the Ti<sub>2</sub>O<sub>3</sub><sup>+</sup> signal. The total etching ion dose applied was approximately 10<sup>17</sup> ions/cm<sup>2</sup>. Note that from the optical image shown in Fig. 1(c), the shell thickness of the sphere is approximately 1/10 of the diameter of the sphere. As in this case the diameter of the sphere is ~20 μm, the thickness of the shell is ~2 μm and the average erosion rate of the TiO<sub>2</sub> microsphere is approximately 2 nm<sup>3</sup>/C<sub>60</sub><sup>+</sup> primary ion, a value close to the reported erosion rates of other inorganic materials.<sup>[30]</sup>

In addition, three consecutive images were taken before and after the etching process with the same ion fluence, approximately 10<sup>13</sup> ions/cm<sup>2</sup> per image. One image of each is shown in Fig. 7, along with the Ti<sub>2</sub>O<sub>3</sub><sup>+</sup> signal level in the bombarded area. The data in Fig. 7 show that the Ti<sub>2</sub>O<sub>3</sub><sup>+</sup> signal is in a steady state before the bombardment. This rules out the possibility that the Ti<sub>2</sub>O<sub>3</sub><sup>+</sup> signal will decay with erosion and demonstrates that SIMS is able to analyze a spherical structure in a layer-by-layer fashion if the structure has a solid core. However, after the bombardment, the signal from Ti<sub>2</sub>O<sub>3</sub><sup>+</sup> disappears in the crater area. At this point, we speculate that the beam started to hit the shell on the opposite side, but the emitted secondary ion cannot be extracted out of the core as a result of the presence of the top of the shell. This observation reinforces the notion that the microsphere has a hollow core. Note that similar results are observed for the other TiO<sub>2</sub>-related signals.

Issues and concerns inherent in this method lie in the complexities of analyzing 2D images of a 3D object, as shown in Fig. 8. This displays the SIMS image of an intact TiO<sub>2</sub> microsphere, where *m/z* 128 for Ti<sub>2</sub>O<sub>2</sub><sup>+</sup> and *m/z* 168 for Si<sub>6</sub><sup>+</sup>

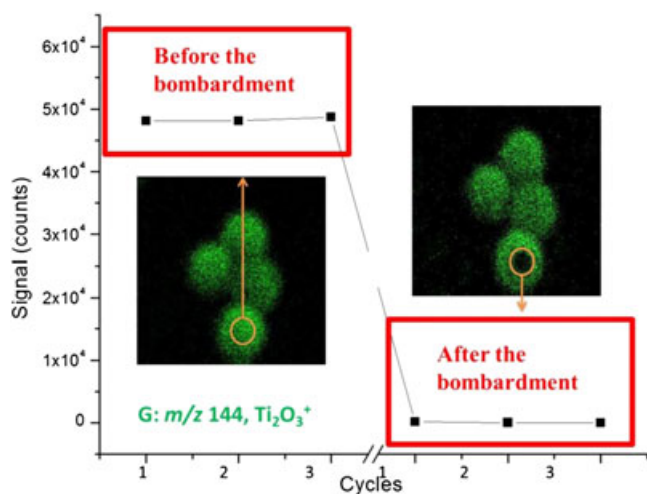


**Figure 7.** Ti<sub>2</sub>O<sub>3</sub><sup>+</sup> signal level in marked region of interest (ROI) before and after the bombardment. The ROI is 5 μm × 5 μm.

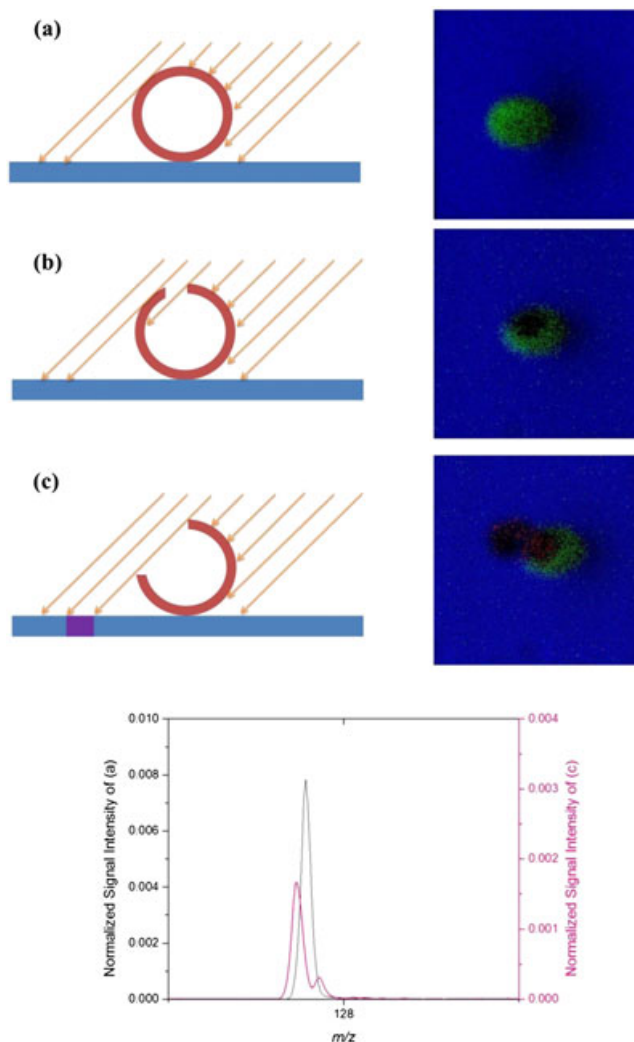


**Figure 8.** Schematic illustration of acquiring SIMS images of TiO<sub>2</sub> microspheres: (a) an intact microsphere; (b) a microsphere with a hole on it; Ti<sub>2</sub>O<sub>2</sub><sup>+</sup> (*m/z* 128, green) and Si<sub>6</sub><sup>+</sup> (*m/z* 168, blue) were used to construct the SIMS images for (a) and (b); (c) a cracked microsphere. The pink color marked the newly revealed area. The inset image shows the split of the Ti<sub>2</sub>O<sub>2</sub><sup>+</sup> (pink) peak in comparison with the one obtained in condition (a) (black). Left and right parts of the split *m/z* 128 peak (green and red) and Si<sub>6</sub><sup>+</sup> (*m/z* 168, blue) were used to construct the SIMS image.

are represented in green and blue, respectively. Note that for the 2D SIMS image, the TiO<sub>2</sub> sphere is elongated into an egg-shape as a result of the incoming beam angle. Next, as described above, the ion beam is left in DC mode to erode a small hole on the surface of the sphere. A SIMS image of the resulting TiO<sub>2</sub> microsphere is shown in Fig. 8(b). Part of the ion beam enters the hole and hits the inside wall of the sphere, but the resulting secondary ions cannot escape since their exit to the extraction field is blocked. As a result, there is a black hole in the TiO<sub>2</sub> sphere image. Finally, the DC beam was used to continue the etching process. As a result, material sputtered from the sphere was deposited in the shadow area (marked in pink). A 256 pixel SIMS image of this deposit is shown in Fig. 8(c). The interesting finding here is

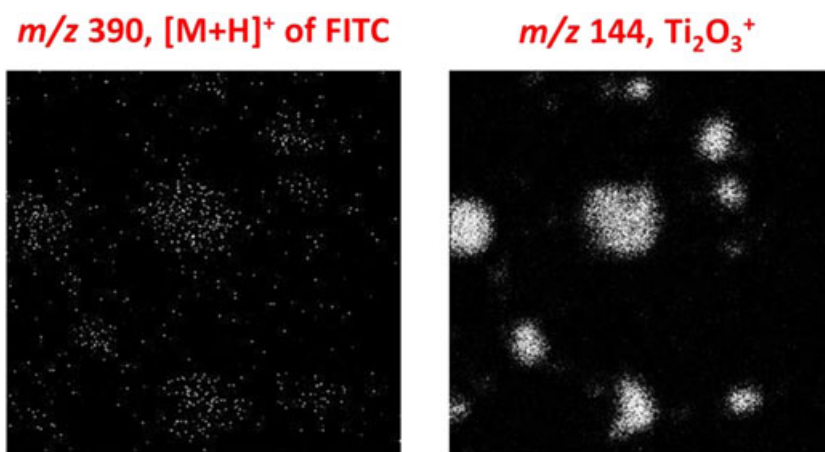


**Figure 9.** Colocalization of the  $[M+H]^+$  ion of the FITC dye and signal from the  $TiO_2$  microspheres. The field of view is  $100\ \mu\text{m} \times 100\ \mu\text{m}$ .

that the  $m/z$  128 peak for  $Ti_2O_2^+$  is split into two regions: the distribution of the left side of the peak is still localized in the sphere region, as in Fig. 8(b), while the distribution of the right side of the peak is localized in the black hole area. The speculation for the origin of the splitting of the peak is that, during the DC etching, part of the eroded materials falls into the flat pink area. Therefore, the time-of-flight of the same material is slightly different due to the sample height difference. Overall, this example shows that the 2D image of a 3D object no longer delivers accurate information about the sample in terms of the exact spatial distribution of the chemical species present in the sample, in both two and three dimensions. It is clear that this problem needs to be addressed for the advancement of this technique and its applications.

#### Surface-modified $TiO_2$ microspheres

Finally, it is of great interest to characterize the fluorescent-labeled hollow  $TiO_2$  microspheres. Similar to the sample transfer procedure described above,  $10\ \mu\text{L}$  of the reaction solution was spin-cast onto a  $5\ \text{mm} \times 5\ \text{mm}$  Si wafer, following which the substrate was rinsed with methanol three times. The extra washing step was used to remove as much ionic liquid as possible, since now the focus of this study is to identify the surface of the microspheres embedded within the ionic liquid. An ion fluence of  $2.0 \times 10^{13}$  ions/ $\text{cm}^2$  was used to take the SIMS image of the fluorescent-labeled sample. Figure 9 clearly demonstrate that SIMS imaging can be used directly to detect the fluorescent dye present on the  $TiO_2$  microspheres. The distribution of the protonated FITC dye ion,  $[M+H]^+$  at  $m/z$  390, is colocalized with that of  $Ti_2O_3^+$  at  $m/z$  144. As shown in Fig. 2(b), upon contact with the  $TiO_2$  microspheres the FITC dye could only react at the surface of the spheres. Therefore, there is only a monolayer of dye molecules attached to the surface of the  $TiO_2$  microspheres, which explains the low level signal observed for the FITC dye. Overall, the finding here is of significance since this model study indicates that SIMS has the potential to map specific markers of monolayers at the submicron level.

## CONCLUSIONS AND PROSPECTS

We have successfully demonstrated that TOF-SIMS can be used to characterize hollow  $TiO_2$  microspheres formed by interfacial sol-gel reactions embedded in an ionic liquid. With the protocols developed here, the scope of such analyses could be expanded to include other systems that use ionic liquids as an embedding medium. One of the ongoing projects in our lab is to characterize liposomes in ionic liquids. Some preliminary data has shown that ionic liquids could be used to help such fragile biological samples maintain their structures under vacuum conditions and imaging mass spectrometry can even capture the phenomenon that liposomes burst under primary ion bombardment (Supplementary Fig. S1, Supporting Information). These findings may lead to the use of TOF-SIMS for the study of model drug release systems. In addition, we have shown some problems associated with imaging SIMS in this study, where complexities arise from projecting a 3D object into a 2D image plane. More fundamental studies on this hollow microsphere model will probably provide a clue as to how to address these problems.

## Acknowledgements

This study was financially supported by the National Institutes of Health (Grant No. 9R01 GM113746-20A1). In addition, infrastructure support from the National Science Foundation (under Grant No. CHE-12-12645) and by the Division of Chemical Sciences at the Department of Energy (Grant No. DE-FG02-06ER15803) is acknowledged.

## REFERENCES

- [1] A. P. Minton. How can biochemical reactions within cells differ from those in test tubes? *J. Cell Sci.* **2015**, *128*, 1254.
- [2] J. M. Anderson. Biological responses to materials. *Annu. Rev. Mater. Res.* **2001**, *31*, 81.

- [3] K. E. Sapsford, W. R. Algar, L. Berti, K. B. Gemmill, B. J. Casey, E. Oh, M. H. Stewart, I. L. Medintz. Functionalizing nanoparticles with biological molecules: Developing chemistries that facilitate nanotechnology. *Chem. Rev.* **2013**, *113*, 1904.
- [4] R. A. Sperling, W. J. Parak. Surface modification, functionalization and bioconjugation of colloidal inorganic nanoparticles. *Philos. Trans. R. Soc. A* **2010**, *368*, 1333.
- [5] D. Touboul, F. Kollmer, E. Niehuis, A. Brunelle, O. Lapr evote. Improvement of biological time-of-flight-secondary ion mass spectrometry imaging with a bismuth cluster ion source. *J. Am. Soc. Mass Spectrom.* **2005**, *16*, 1608.
- [6] N. Winograd. The magic of cluster SIMS. *Anal. Chem.* **2005**, *77*, 142 A.
- [7] A. G. Shard, R. Havelund, M. P. Seah, S. J. Spencer, I. S. Gilmore, N. Winograd, D. Mao, T. Miyayama, E. Niehuis, D. Rading, R. Moellers. Argon cluster ion beams for organic depth profiling: Results from a VAMAS interlaboratory study. *Anal. Chem.* **2012**, *84*, 7865.
- [8] B. Liu, X.-Y. Yu, Z. Zhu, X. Hua, L. Yang, Z. Wang. In situ chemical probing of the electrode-electrolyte interface by ToF-SIMS. *Lab Chip* **2014**, *14*, 855.
- [9] D. Breitenstein, C. E. Rommel, R. Mollers, J. Wegener, B. Hagenhoff. The chemical composition of animal cells and their intracellular compartments reconstructed from 3D mass spectrometry. *Angew. Chem. Int. Ed.* **2007**, *46*, 5332.
- [10] M. A. Robinson, D. J. Graham, D. G. Castner. ToF-SIMS depth profiling of cells: z-correction, 3D imaging, and sputter rate of individual NIH/3 T3 fibroblasts. *Anal. Chem.* **2012**, *84*, 4880.
- [11] H. Nygren, B. Hagenhoff, P. Malmberg, M. Nilsson, K. Richter. Bioimaging TOF-SIMS: High resolution 3D imaging of single cells. *Microsc. Res. Techniq.* **2007**, *70*, 969.
- [12] A. M. Piwowar, S. Keskin, M. O. Delgado, K. Shen, J. J. Hue, I. Lanekoff, A. G. Ewing, N. Winograd. C60-ToF SIMS imaging of frozen hydrated HeLa cells. *Surf. Interface Anal.* **2013**, *45*, 302.
- [13] J. S. Fletcher, N. P. Lockyer, S. Vaidyanathan, J. C. Vickerman. TOF-SIMS 3D biomolecular imaging of *Xenopus laevis* oocytes using buckminsterfullerene (C-60) primary ions. *Anal. Chem.* **2007**, *79*, 2199.
- [14] S. G. Ostrowski, C. T. Van Bell, N. Winograd, A. G. Ewing. Mass spectrometric imaging of highly curved membranes during tetrahymena mating. *Science* **2004**, *305*, 71.
- [15] Z. Takats, J. M. Wiseman, B. Gologan, R. G. Cooks. Mass spectrometry sampling under ambient conditions with desorption electrospray ionization. *Science* **2004**, *306*, 471.
- [16] J. M. Wiseman, D. R. Ifa, Q. Song, R. G. Cooks. Tissue imaging at atmospheric pressure using desorption electrospray ionization (DESI) mass spectrometry. *Angew. Chem. Int. Ed.* **2006**, *45*, 7188.
- [17] J. M. Wiseman, D. R. Ifa, Y. Zhu, C. B. Kissinger, N. E. Manicke, P. T. Kissinger, R. G. Cooks. Desorption electrospray ionization mass spectrometry: Imaging drugs and metabolites in tissues. *Proc. Natl. Acad. Sci.* **2008**, *105*, 18120.
- [18] R. D. Rogers, K. R. Seddon. Ionic liquids – Solvents of the future? *Science* **2003**, *302*, 792.
- [19] T. Welton. Room-temperature ionic liquids. Solvents for synthesis and catalysis. *Chem. Rev.* **1999**, *99*, 2071.
- [20] P. Wasserscheid, W. Keim. Ionic liquids – New "solutions" for transition metal catalysis. *Angew. Chem. Int. Ed.* **2000**, *39*, 3772.
- [21] J. Dertinger, A. Walker. Ionic liquid matrix-enhanced secondary ion mass spectrometry: The role of proton transfer. *J. Am. Soc. Mass Spectrom.* **2013**, *24*, 348.
- [22] J. J. D. Fitzgerald, P. Kunnath, A. V. Walker. Matrix-enhanced secondary ion mass spectrometry (ME SIMS) using room temperature ionic liquid matrices. *Anal. Chem.* **2010**, *82*, 4413.
- [23] J. Dertinger, A. Walker. Towards the rational design of ionic liquid matrices for secondary ion mass spectrometry: Role of the anion. *J. Am. Soc. Mass Spectrom.* **2013**, *24*, 1288.
- [24] T. Nakashima, N. Kimizuka. Interfacial synthesis of hollow TiO<sub>2</sub> microspheres in ionic liquids. *J. Am. Chem. Soc.* **2003**, *125*, 6386.
- [25] Q. Y. Qu, H. W. Geng, R. X. Peng, Q. Cui, X. H. Gu, F. Q. Li, M. T. Wang. Chemically binding carboxylic acids onto TiO<sub>2</sub> nanoparticles with adjustable coverage by solvothermal strategy. *Langmuir* **2010**, *26*, 9539.
- [26] N. Nakayama, T. Hayashi. Preparation of TiO<sub>2</sub> nanoparticles surface-modified by both carboxylic acid and amine: Dispersibility and stabilization in organic solvents. *Colloids Surfaces A: Physicochem. Eng. Aspects* **2008**, *317*, 543.
- [27] J. S. Fletcher, S. Rabbani, A. Henderson, P. Blenkinsopp, S. P. Thompson, N. P. Lockyer, J. C. Vickerman. A new dynamic in mass spectral imaging of single biological cells. *Anal. Chem.* **2008**, *80*, 9058.
- [28] H. Seiler. Secondary electron emission in the scanning electron microscope. *J. Appl. Phys.* **1983**, *54*, R1.
- [29] K. Shen, D. Mao, B. J. Garrison, A. Wucher, N. Winograd. Depth profiling of metal overlayers on organic substrates with cluster SIMS. *Anal. Chem.* **2013**, *85*, 10565.
- [30] R. J. Paruch, B. J. Garrison, Z. Postawa. Computed molecular depth profile for C60 bombardment of a molecular solid. *Anal. Chem.* **2013**, *85*, 11628.

## SUPPORTING INFORMATION

Additional supporting information may be found in the online version of this article at the publisher's website.